The generation, characterization and applications of broadband isolated attosecond pulses

Michael Chini, Kun Zhao and Zenghu Chang*

The generation of extremely short isolated attosecond pulses requires both a broad spectral bandwidth and control of the spectral phase. Rapid progress has been made in both aspects, leading to the generation of light pulses as short as 67 as in 2012, and broadband attosecond continua covering a wide range of extreme ultraviolet and soft X-ray wavelengths. Such pulses have been successfully applied in photoelectron and photoion spectroscopy and recently developed attosecond transient absorption spectroscopy to study electron dynamics in matter. In this Review, we discuss significant recent advances in the generation, characterization and applications of ultrabroadband, isolated attosecond pulses with spectral bandwidths comparable to the central frequency. These pulses can in principle be compressed to a single optical cycle.

Since the first demonstration of isolated attosecond pulses by high-order harmonic generation (HHG) in 2001[1], the extension of time-resolved spectroscopy to the attosecond domain has greatly enhanced our understanding of ultrafast electronic processes in atoms, molecules and condensed matter. Much of this progress has occurred in the past several years as a result of the proliferation of attosecond technology in many laboratories around the world, as well as the maturation of attosecond spectroscopic techniques. Just as the extension of high-power femtosecond laser pulses to the few-optical-cycle regime in the 1990s[2] opened new avenues in strong-field physics and directly led to the 'attosecond revolution'[3], the development and application of attosecond light sources is expected to similarly inspire new breakthroughs in ultrafast science.

Few-cycle optical pulses require ultrabroad spectral bandwidths that are comparable to or even larger than the central frequency, as well as accurate characterization and control of the spectral phase. Fully harnessing attosecond science will ideally allow the generation of few- or even single-cycle optical pulses — currently possible at visible and infrared wavelengths by chirped pulse amplification and optical parametric amplification — to be extended to the extreme-ultraviolet (XUV) and soft X-ray (SXR) spectral regions. Presently, however, the shortest achievable isolated attosecond pulses (67 as; ref. 4) are still significantly longer than those supported by the broadest attosecond supercontinuum spectra (Fourier-transform-limited pulse duration, 16 as; ref. 5). This discrepancy, detailed in Table 1, results not only from the difficulty of generating ultrabroadband attosecond supercontinua, but also from the difficulty of characterizing and compensating the spectral phase over such a broad bandwidth and ultimately delivering the compressed pulse to a target for applications. The development of new techniques for generating, characterizing and applying broadband, isolated attosecond pulses is therefore crucial for the advancement of attosecond science.

In this Review, we describe recent progress in the development of broadband, isolated attosecond sources, supporting few- or single-cycle XUV pulses. Although such few-cycle pulses have been demonstrated with central energies of 35 eV (ref. 6), 80 eV (ref. 7) and 90 eV (ref. 4), the technology is still relatively immature, and new techniques are needed to make the next significant advances. This Review reports on the most recent progress in the generation, characterization and application of broadband isolated attosecond pulses. In particular, we focus on those techniques that can be applied to ultrabroadband pulses, which are ideally compressible to a single optical cycle and which hold significant promise for the extension of attosecond science to shorter pulse durations. The Review also covers the current state of the art for applications of broadband isolated attosecond pulses to the study of bound electron dynamics and to the measurement and control of correlated systems.

Generating ultrabroadband attosecond pulses

HHG naturally results in the generation of attosecond pulse trains with ultrabroad spectral bandwidths in the XUV and SXR spectral regions, characterized by a relatively flat 'plateau' spectrum extending from below a target atom's ionization threshold[8,9] to the high-harmonic cutoff. The harmonic cutoff photon energy is proportional to the driving laser intensity I before the atom is fully ionized. It is also proportional to the square of the driving laser wavelength λ, and can thus extend into the 'water window' region of X-ray transmission[10,11] when driven by intense Ti:sapphire laser pulses ($\lambda \approx 800$ nm) and beyond 1 keV with longer wavelength drivers[12,13]. Generation of ultrabroadband attosecond pulses is therefore achievable only by making use of the full high-order harmonic spectrum, including both the plateau and cutoff harmonics. Isolated attosecond pulses produced by HHG have been experimentally demonstrated and characterized using a variety of experimental techniques (most of which have been covered extensively in previous reviews[3,14–16]); these include spectral selection of half-cycle cutoffs[17–19] as in amplitude gating[7,20,21] and ionization gating[22–25], temporal gating techniques such as polarization gating[6,26,27] and double optical gating (DOG)[4,28–30], and spatiotemporal gating with the attosecond lighthouse effect[31,32].

Of these, only the polarization gating, DOG and attosecond lighthouse techniques are suitable for generating ultrabroadband attosecond pulses, as illustrated in Fig. 1. In spectral selection techniques, such as amplitude gating (Fig. 1a) and ionization gating (Fig. 1b), only the attosecond pulse produced by the most intense half cycle of the laser (or the most intense half cycle before ground-state depletion, in the case of ionization gating) produces the cutoff spectral components with the highest photon energies (blue shading), whereas the low-energy spectral components (red shading) arise from multiple attosecond pulses produced by other half cycles of the driving laser field with lower amplitude. Extracting an isolated attosecond pulse from the attosecond pulse train therefore requires that the highly modulated low-energy spectral components originating from interference of two or more

Institute for the Frontier of Attosecond Science and Technology (iFAST), CREOL and Department of Physics, University of Central Florida, Orlando, Florida 32816, USA. *e-mail: zenghu.chang@ucf.edu

Table 1 | State of the art in ultrabroadband isolated attosecond pulse generation, compression and characterization.

Gating method	Gas	Central energy (eV)	FWHM bandwidth (eV)	FT limit (as)	Measured duration (as)	Compression method	Characterization method	Refs
Amplitude gating	Ne	80	28	75	80	Zr foil	FROG-CRAB	7
Ionization gating	Xe	25	8	130	155	Al foil	FROG-CRAB	25
Polarization gating	Ne	100	22	45	130*	Al foil	FROG-CRAB	6, 41
DOG	Ne	100	170	16	67	Zr foil, phase matching	PROOF	4, 5
Interferometric PG	Kr	26	15	260	N/A	None	N/A	44
Generalized DOG	He	200	60	20	148*	Al foil	FROG-CRAB	29, 46
Attosecond lighthouse	Ne	50	35	47	N/A	None	N/A	32

*The pulse durations for polarization gating and generalized DOG were measured using attosecond pulses generated in Ar gas. PG, polarization gating, FWHM, full-width at half-maximum; FT, Fourier transform.

attosecond pulses (Fig. 1e) be blocked by a suitable filter that transmits only the attosecond continuum spectrum at the cutoff. Such schemes preclude the generation of isolated attosecond pulses with ultrabroad bandwidths, because the usable cutoff spectrum (yellow shading) typically covers a relatively small portion of the total XUV/SXR spectrum. This limitation can in principle be overcome by the development of half-cycle near-infrared (NIR) driving pulses through field synthesis of light transients[33,34]. Currently, however, even state-of-the-art laser pulses with a full-width at half-maximum pulse duration of 2.1 fs (~0.9 optical cycles)[33] are too long to suppress completely the attosecond emission from multiple half cycles. On the other hand, the polarization gating, DOG (Fig. 1c) and attosecond lighthouse (Fig. 1d) techniques make use of both the plateau and cutoff spectral components, resulting in an ultrabroadband attosecond supercontinuum (Fig. 1f).

Temporal gating. Generation of broadband isolated attosecond pulses requires an attosecond 'light switch' — a technique that can effectively turn on the HHG process during only a single half cycle of the driving laser field, with the carrier-envelope phase (CEP) of the driving laser set so that only electron trajectories originating from a single ionization event (electric-field maximum) result in attosecond pulse generation. To date, the most effective switches are based on the polarization gating technique. Attosecond pulses can be generated efficiently when the driving laser field is linearly polarized, as explained by the semiclassical recollision model[35]. However, the conversion efficiency drops rapidly when the driving laser is elliptically or circularly polarized[26,36,37]. The efficiency of attosecond pulse generation decreases by ~50% when the ellipticity is increased from 0 to only 0.1 (ref. 27), and by about an order of magnitude for an ellipticity of 0.2. Therefore, a single attosecond pulse can be isolated if a driving laser can be produced that generates pulses that are linearly polarized during a single half cycle and elliptically polarized during the remainder of the pulse.

The driving pulse for polarization gating can be produced by combining two counter-rotating circularly polarized few-cycle laser pulses that have a certain time delay between them[6,27,38,39]. For a suitably chosen delay[40], the resulting pulse will be linearly polarized only during the central half cycle, with circularly polarized leading and trailing edges. The CEP dependence of the attosecond spectrum exhibits a π periodicity, as one or two attosecond pulses can be emitted within the gate depending on the CEP. In 2009, ultrabroadband attosecond continua were generated using polarization gating with a spectral coverage of 60–140 eV, and supporting a transform-limited pulse duration below 50 as (ref. 41), which is approaching the atomic unit of time. The primarily limitation

of the polarization gating technique for the generation of even broader attosecond supercontinua by extending the spectral cutoff is the reduction in the attosecond-pulse-generation efficiency as a result of the depletion of the target-atom ground state with increasing laser intensity. For ~5 fs driving lasers, the required delay between the two circularly polarized pulses is comparable to the laser pulse duration, and the ground state of the target atom can be fully depleted before the linear gate. Further reduction of the pulse duration would allow the use of higher driving laser intensities, but this is extremely difficult.

This limitation of polarization gating can be overcome by the addition of a linearly polarized second-harmonic field to the driving field with time-dependent ellipticity. In the asymmetric two-colour field, attosecond pulse generation occurs only once per optical cycle[42,43], instead of once every half cycle, and the polarization gate can remain open for a full optical cycle. This technique is known as double optical gating[28]. This means that, for the same input pulse duration, the delay between the two elliptically polarized pulses can be reduced by a factor of two. This in turn reduces the probability that the target atom will be ionized before the gate, allowing higher laser intensities to be used. As the ionization rate is highly nonlinear with respect to the driving laser intensity, the DOG technique allows a significantly higher driving laser intensity to be used than for polarization gating with the same pulse duration. The field asymmetry also results in a 2π periodicity of the attosecond pulse spectrum with the CEP. In 2009, attosecond supercontinuum spectra were generated from 8 fs driving lasers with an in-gate intensity of 1.4×10^{16} W cm^{-2} using the DOG technique, yielding a nearly 200 eV full-width at half-maximum bandwidth supporting 16-as transform-limited pulses[5]. This is the broadest attosecond supercontinuum spectrum generated to date. By extending the DOG technique to 5 fs pulses, which are now available in many laboratories, DOG can be used with higher intensities; the cutoff is thus expected to be further extended.

Another critical advance in the generation of ultrabroadband attosecond pulses has come with the development of the interferometric polarization gating[44] and generalized DOG[29] techniques, for which the driving laser pulse has elliptically (rather than circularly) polarized leading and trailing edges. Because the polarization gate width is directly proportional to the ellipticity ε of the pulse, the use of elliptical (say, $\varepsilon = 0.5$) rather than circular ($\varepsilon = 1$) polarization can allow the generation of isolated attosecond pulses from longer driving lasers[29,45] or reduce the ground state depletion when high-intensity, few-cycle pulses are used[46]. In addition to allowing further extension of the attosecond supercontinuum cutoff with higher intensity few-cycle driving lasers, the generalized DOG technique also holds
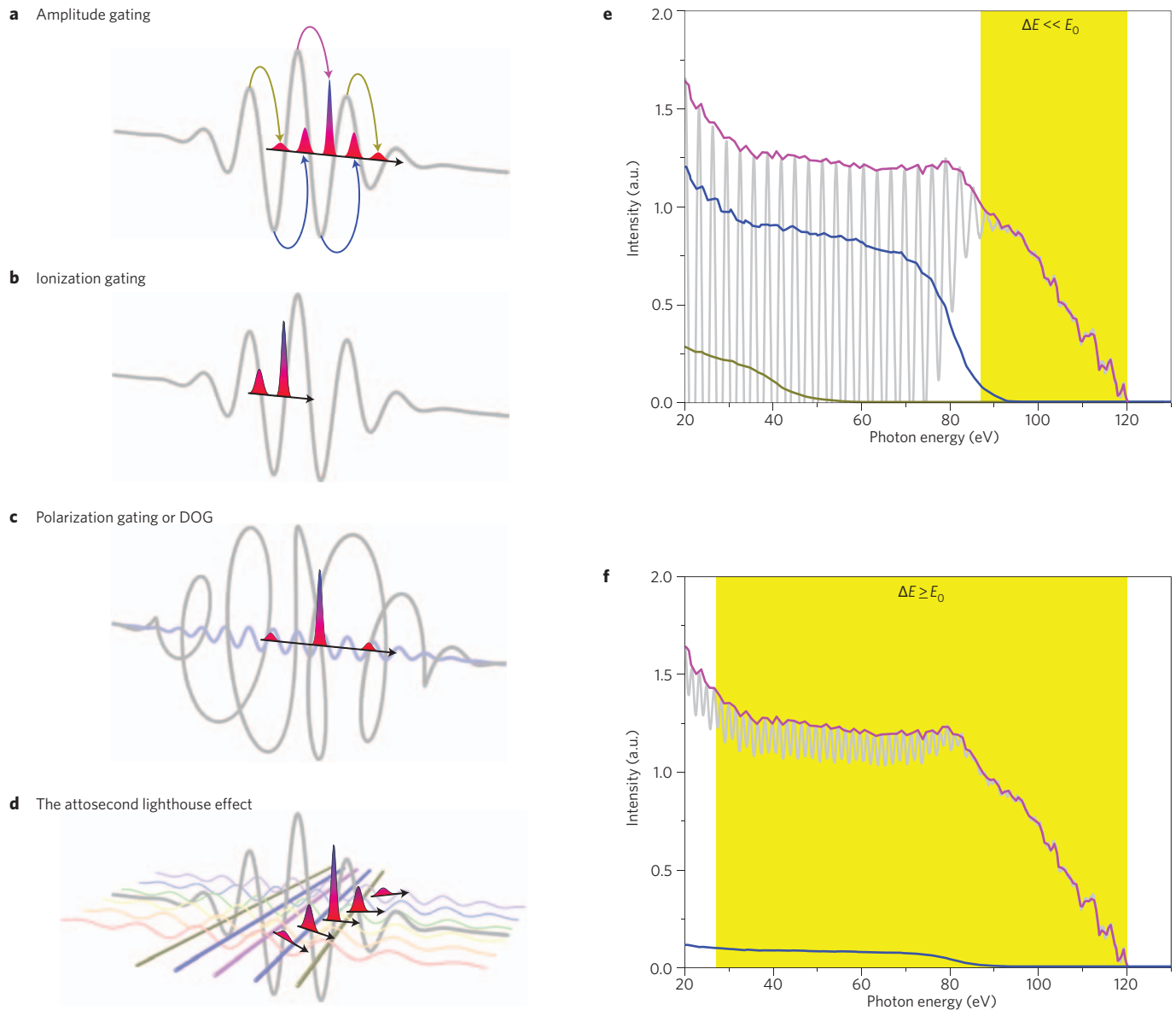
179

Figure 1 | Gating an ultrabroadband isolated attosecond pulse. Various techniques have been demonstrated for generating isolated attosecond pulses: **a**, Amplitude gating; **b**, ionization gating; **c**, polarization gating or DOG; **d**, the attosecond lighthouse effect. **e,f** Only the cutoff spectrum is usable with amplitude gating or ionization gating (**e**); polarization gating, DOG and the attosecond lighthouse effect can produce ultrabroadband attosecond pulses with a continuum spectrum covering the plateau and cutoff (**f**). The magenta, blue, and green lines indicate the contributions of different half cycles to the total attosecond spectrum.

promise for the development of high-flux ultrabroadband attosecond pulses when combined with high-energy driving laser pulses[47].

Spatiotemporal gating. Another promising route for the generation of ultrabroadband isolated attosecond pulses is the attosecond light-house effect[31]. Whereas previous gating techniques have primarily made use of time-dependent laser waveforms, the attosecond light-house effect is the first to take advantage of spatiotemporal coupling in the driving laser field. In particular, it relies on the driving laser field exhibiting wavefront rotation in order to generate angularly sep-arated attosecond pulses. Normally, when a laser pulse is used to drive HHG, the attosecond pulses are emitted in a spatially confined beam, which typically has a much lower divergence than the driving laser beam. On the other hand, when generated by a rotating wavefront, each attosecond pulse in the train will be emitted in a different direc-tion — perpendicular to the instantaneous wavefront of the driving

laser at the time of its generation. Therefore, if the wavefront rota-tion within one half cycle of the driving laser field is larger than the divergence of the attosecond pulse, the attosecond lighthouse effect can result in the generation of an isolated attosecond pulse by spatial selection in the far field. The attosecond lighthouse effect is character-ized by its unique dependence on the driving laser CEP — for differ-ent CEP values, the propagation direction of the attosecond pulse will change, as the attosecond pulse is generated at a different location in the rotating wavefront.

The attosecond lighthouse effect has been demonstrated experi-mentally in harmonics generated from a plasma mirror[48] and from a neon gas target[32]. In both cases, the isolated attosecond pulse is indi-cated by a spectrum that is continuous over its entire bandwidth and by the carrier-envelope phase dependence. In particular, for the gas-phase harmonics, the continuum spectrum covers both the plateau and cutoff orders of the high-order harmonic spectrum, extending
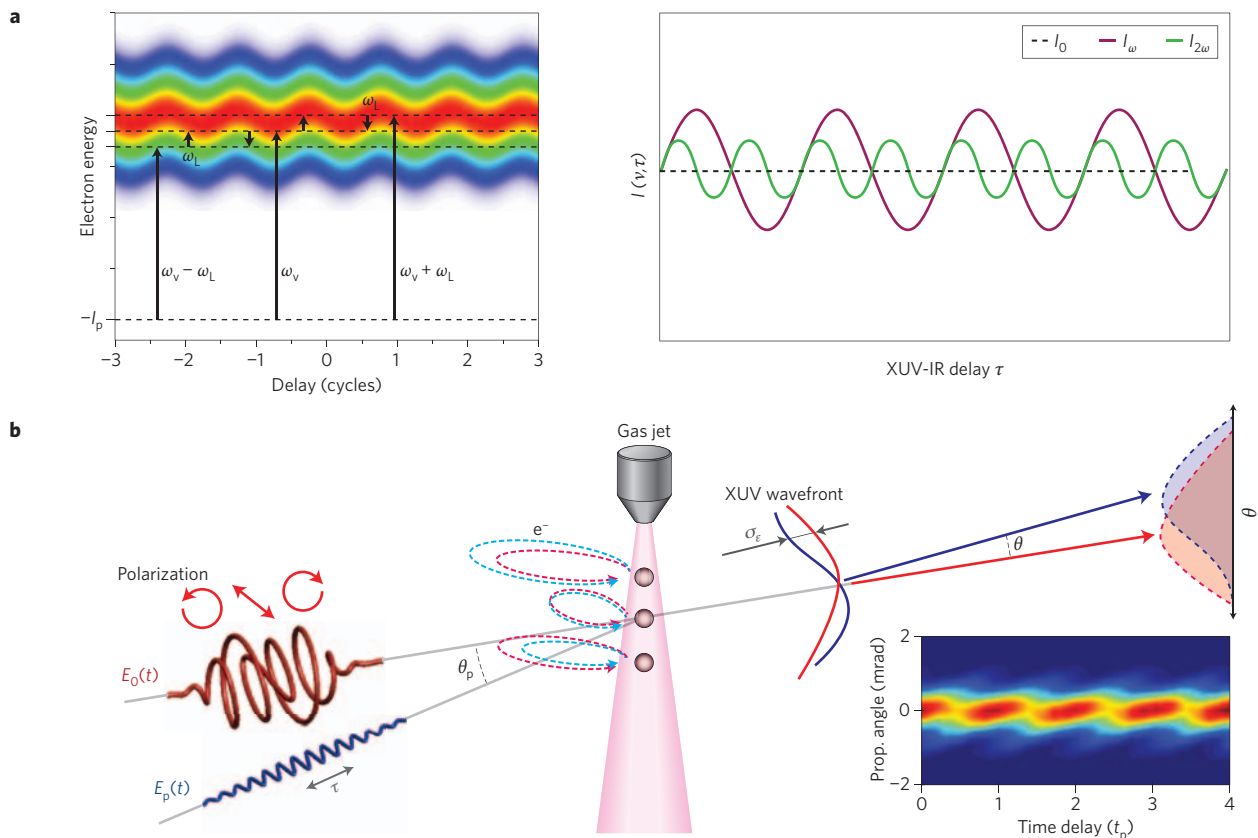
Figure 2 | Attosecond pulse characterization. Temporal measurements on ultrabroadband attosecond pulses necessitate methods that do not require narrow-bandwidth approximations. **a**, In PROOF, the weak perturbation of the dressing NIR laser field imprints an interference oscillation on measured delay-dependent photoelectron momentum spectrum. **b**, *In situ* characterization relies on a weak perturbation to the attosecond pulse generation, resulting in an angular deflection of the attosecond beam that can be measured in the far field. Figure reproduced with permission from: **a**, ref. 63, © 2010 OSA and ref. 68, © 2013 OSA; **b**, ref. 72, © 2013 NPG.

from 30 eV to more than 110 eV. Extension of the attosecond light-house effect to even broader bandwidths is relatively straightforward, as the divergence angle of the attosecond pulse tends to decrease with increasing photon energy, allowing cleaner selection of the isolated attosecond pulse.

Extension to mid-infrared driving lasers. In principle, every gating technique for generating ultrabroadband attosecond pulses could benefit from the use of few-cycle, mid-infrared laser sources. This is primarily because of the well-known increase in the cutoff photon energy[12,49,50] with increasing λ^2, which allows broader bandwidths to be realized than with Ti:sapphire lasers. Additionally, recent studies have revealed that using such sources reduces the attosecond frequency chirp[51] (proportional to λ^{-1}) and improves the phase matching[13,52,53], which will be critical for the development of high-flux attosecond X-ray sources. Recent improvements in the infrastructure for optical parametric amplification and optical parametric chirped pulse amplification with spectra between 1.3 μm and 4 μm (refs 54–59) have led to several major advances in the generation of broadband high-harmonic spectra[13,60,61]. However, the appearance of a continuum spectrum in such experiments is probably an experimental artefact, as the grating spectrometer has insufficient resolution to resolve the narrow spacing of high-order harmonics from mid-infrared lasers; the dependence of the spectrum on the driving laser CEP has yet to be demonstrated.

Characterizing ultrabroadband attosecond pulses
Characterization of broadband isolated attosecond pulses is also

challenging. Nonlinear autocorrelation methods, which have been extremely successful in femtosecond science, cannot be straight-forwardly extended to the attosecond domain, as a result of both the lack of effective nonlinear materials in the XUV/SXR spectral region and the low photon flux of attosecond pulses. Instead, attosecond spectroscopy has relied on pulse characterization methods that combine the attosecond pulse with a delayed NIR laser field. This forms the basis of the frequency-resolved optical gating for complete reconstruction of attosecond bursts (FROG-CRAB) technique[62] in which the attosecond spectral phase is encoded in laser-induced perturbations to the kinetic momentum spectrum of an electron replica of the attosecond pulse. Although the FROG-CRAB technique has been widely applied to the characterization of isolated attosecond pulses and attosecond pulse trains, it is not suited for the characterization of ultrabroadband attosecond pulses, as the reconstruction algorithm relies on a narrow-bandwidth approximation[63,64]; alternative methods are thus needed.

Phase retrieval by omega oscillation filtering. In the FROG-CRAB technique, the combined action of the attosecond pulse and the delayed NIR dressing laser ionizes an atomic target, yielding a delay-dependent photoelectron energy spectrum. Extracting the attosecond pulse duration from such a spectrogram is nontrivial and requires approximate analytical descriptions of the laser-dressed photoionization process. In the case of the FROG-CRAB technique, the spectral bandwidth is assumed to be narrow (known as the central momentum approximation in the literature). Under this assumption, the spectrum has the mathematical form of a FROG
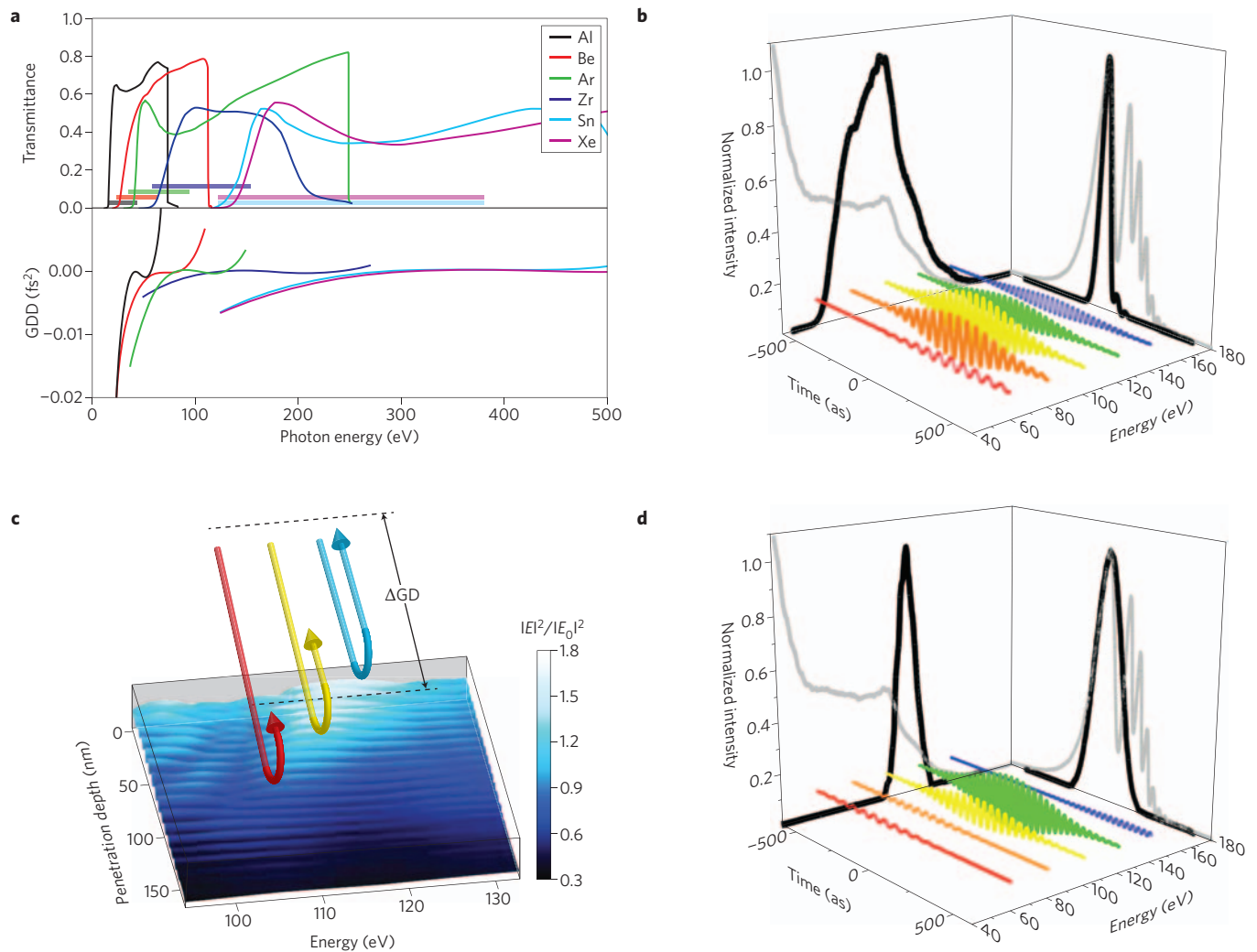
Figure 3 | Conventional methods for attosecond pulse compression. a, Various metal-foil filters have transmission and a negative GDD over a relatively broad energy range. **b,** Spectrum and temporal profile before (grey lines in projections) and after (black lines in projections) passing through the Zr-foil filter. The attosecond chirp is compensated so that different frequency components (coloured lines in the three-dimensional image) of the attosecond pulse add in phase to generate a short pulse. **c,** In a chirped multilayer mirror, different frequency components of the attosecond pulse (coloured lines) penetrate to different depths within the mirror, imprinting a change in the group delay across the reflected spectrum. **d,** Chirped mirrors currently have limited bandwidth, but are more flexible than metal-foil filters. Figure reproduced with permission from: **a,** ref. 76, © 2012 IOP; **c,** ref. 79, © 2011 OSA.

trace, allowing reliable FROG retrieval algorithms to be used[64,65]. For ultrabroadband attosecond pulses, however, a different approximation must be made to ensure the accurate retrieval of the spectral phase over the entire spectral bandwidth. For this reason, phase retrieval by omega oscillation filtering (PROOF) was developed[63]. Like the FROG-CRAB technique, PROOF relies on the measurement of electrons photoionized by an attosecond pulse under the perturbation of a dressing laser field. In this case, the dressing laser is assumed to be weak, and can thus be treated using lowest-order perturbation theory, similar to the reconstruction of attosecond beating by interference of two-photon transitions (RABITT) technique for characterizing attosecond pulse trains[66].

When the interaction of the XUV/SXR and NIR laser pulses with the target atom is treated in the framework of second-order perturbation theory, the yield of photoelectrons with a fixed momentum v oscillates with the time delay. The resulting photoelectron momentum spectrum $I(v, \tau)$ can then be written as a sum of three components: $I(v, \tau) = I_0(v) + I_\omega(v, \tau) + I_{2\omega}(v, \tau)$, as illustrated in Fig. 2a. Here, I_0 represents the combined probability of one-photon

(XUV/SXR) and two-photon (XUV/SXR + NIR) absorption, and does not depend on the delay. I_ω and $I_{2\omega}$ result from interferences between the different one- and two-photon pathways to a given final state, and oscillate with the delay τ at the NIR laser frequency ω and at 2ω, respectively. Because the attosecond pulse imprints its spectral phase on the photoelectron replica, the spectral phase differences between the interfering pathways are encoded in the time delay dependence of I_ω, and can be extracted using a suitable algorithm[4,63,67,68].

***In situ* characterization.** Temporal characterization of the attosecond emission can also be performed within the generation medium itself by extending an experimental technique pioneered by Dudovich *et al.* for characterizing the emission time of different high-order harmonics in an attosecond pulse train[69]. In this *in situ* method, a weak second-harmonic field is added to the driving field for HHG with a variable time delay. Although the second-harmonic perturbation is relatively weak, it can result in measurable changes to the spatial[70] and spectral[42] character of the
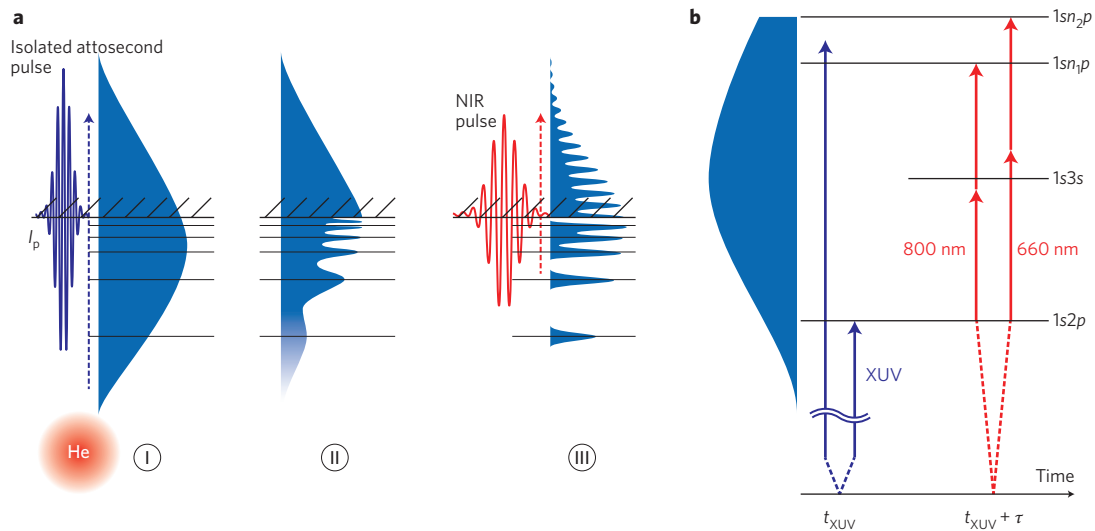
Figure 4 | Schematic of attosecond electron interferometry and attosecond transient absorption measurements in helium. a, In attosecond electron interferometry, an isolated attosecond pulse excites the helium atom to both bound and continuum states (I). These states freely evolve in time (II) until the arrival of a delayed NIR laser pulse (III), which ionizes the bound excited states. Interferences between the two ionization pathways are measured in the photoelectron spectrum. **b**, In attosecond transient absorption, additional features can be observed as a result of bound–bound coupling, for example between the 1s2p, 1s3s, and 1snp states. Figure reproduced with permission from: **a**, ref. 82, © 2010 APS; **b**, ref. 90, © 2013 APS.

attosecond emission. Here, the addition of the second harmonic breaks the half-cycle symmetry of the driving laser field, resulting in the generation of both odd and even harmonic orders. The yield of a given even harmonic depends on both the subcycle time delay between the fundamental and second-harmonic fields and the harmonic emission time, and it oscillates with the time delay between the two fields. Similarly to the PROOF technique, this oscillation can be interpreted as an interference arising from different quantum pathways, resulting in the emission of the same even harmonic[71], and the emission times (spectral phases) of the different harmonics can be extracted from the phase of the oscillation. Such interferences are largely independent of the harmonic photon energy, and the technique can be extended to ultrabroad spectral bandwidths. Moreover, as an all-optical technique, its measurement time can be made dramatically lower than PROOF and other photoelectron measurement techniques.

Until recently, the *in situ* technique relied on the measurement of discrete even harmonics, limiting its applicability to the measurement of the intrinsic frequency chirp of attosecond pulse trains[51,71]. However, the technique has now been extended to the characterization of isolated attosecond pulses by exploiting spatiotemporal coupling of the two laser fields, resulting in measurable changes to the spatially and spectrally resolved attosecond pulse. When the weak second-harmonic field $E_p(t)$ is introduced to the generation medium at a small angle θ_p with respect to the driving field $E_0(t)$, the spatiotemporal coupling of the two pulses modifies the XUV/SXR wavefront and causes an angular deflection of the attosecond pulse's propagation direction[72], as illustrated in Fig. 2b. Measurement of the spatial profile of the generated beam as a function of both the XUV/SXR photon energy and the time delay between the fundamental and second-harmonic pulses allows full space–time characterization of the amplitude and phase of the attosecond pulse in the generation medium, and, by extension, at all points in space. Although the *in situ* technique cannot be used to determine directly the temporal profile of the attosecond pulse when delivered to a secondary target, it can be used to inform accurately the design of attosecond compression techniques to deliver ultimately single-cycle attosecond pulses with ultrabroad bandwidths.

Attosecond pulse compressors

The primary goal in generating ultrabroadband spectra is to take advantage of the full spectral bandwidth, yielding ultrashort attosecond pulses at the single-optical-cycle level. Several techniques have recently been demonstrated that give promising results on this front, but there is still no 'catch-all' technique that provides both ultrabroad bandwidths and complete compensation of the phase error. Here, we focus on those techniques that have been successfully implemented experimentally, although several theoretical proposals show promise for eliminating the intrinsic chirp of attosecond pulses in the generation medium through coherent field synthesis[73,74].

Foil filters. The HHG process intrinsically imprints a positive frequency chirp on the emitted attosecond pulse, as high-energy photons are emitted slightly after those with lower energy. Within the plateau, this leads to a group delay which increases linearly with increasing photon energy. This positive chirp can be compensated by the negative group delay dispersion (GDD) of a suitably chosen foil filter[75,76], as illustrated in Fig. 3a,b. Unfortunately, this compression scheme is extremely limited — although foil filters are available with transmission windows and a negative GDD in a variety of spectral regions, their transmission bandwidths are not tunable and generally do not approach the full bandwidth of the attosecond supercontinuum. Moreover, the overall transmission is low, and spectral phase distortions near the edges of the transmission windows tend to lengthen the attosecond pulse duration. However, foil filters are still the most successful method for compressing attosecond pulses, having first been used to demonstrate compression to a single cycle in 2006[6], and they remain a staple of attosecond technology today.

Chirped multilayer mirrors. Another approach to compressing attosecond pulses is the extension of chirped multilayer mirror technology from the visible/NIR spectral region to the XUV/SXR region. Multilayer mirrors have long been implemented in high-order harmonic beamlines because of their relatively high reflectivity at normal incidence; indeed, they were applied as focusing optics in the first attosecond experiments[1]. However, despite

early proposals to use chirped multilayer mirrors to compensate the spectral phase of high-order harmonics[77,78], such mirrors were predominantly used in conjunction with metal-foil filters, with the mirrors serving only as band-pass filters, rather than aiding compression (as in the characterization of 80 as pulses reported in 2008[7]). The first chirped mirrors for attosecond pulses were realized in 2011[79], with a reflectivity as high as 10% in a spectral bandwidth of 100–130 eV, supporting transform-limited pulse durations of 165 as. In the chirped mirror, different frequency components of the attosecond pulse penetrate to different depths within the mirror before reflection, resulting in different spectral components having different group delays, as illustrated in Fig. 3c,d. Although chirped multilayer mirrors are currently available only with limited spectral bandwidth, rapid progress is being made in their design, manufacture and characterization. Already, chirped multilayer mirrors have been proposed that are capable of compressing 70 as pulses with a spectral range of 300–350 eV (ref. 80) and sub-50 as pulses with a spectral range of 20–112 eV (ref. 81). Chirped multilayer mirrors supporting ultrabroad bandwidths will probably become available in the coming years as further technical advances are made.

Single-cycle attosecond pulses. Reliably compressing ultrabroadband attosecond pulses to the single-cycle limit in a wide wavelength range will require new technologies in attosecond science. Currently, the state of the art in pulse compression relies on combinations of multiple techniques. Generating transform-limited isolated attosecond pulses requires control of the high-energy spectrum and phase, where foil filters have a positive GDD. This can be done by using phase matching to select only the spectral components that have flat phase. Attosecond pulses generated in a dense medium are known to exhibit a reduced cutoff, as a result of poor phase matching at the highest photon energies. Therefore, simply by tuning the pressure in the generation gas target, spectral selection can be used to optimize the attosecond pulse duration without changing the intrinsic chirp or filter properties. This is most easily achieved using a thin (inner diameter is much smaller than the laser confocal parameter) gas cell, although other targets may also be considered. Using such a phase-matched spectral selection, isolated 67 as pulses were produced using DOG[4]. Although reduction of the generation gas pressure leads to measurable broadening of the spectral bandwidth as the cutoff is increased, the pulse duration is expected to increase as a result of the positive filter GDD at higher energies.

Application of ultrabroadband attosecond pulses

Isolated attosecond pulses hold great potential for time-resolved measurements on unprecedented timescales. They will only be realized with the development of high-energy attosecond light sources[16] having ultrabroad bandwidths. Still, broadband isolated attosecond pulses have two major advantages over attosecond pulses generated from the high-order harmonic cutoff: the low-photon-energy plateau spectrum allows access to bound states of atoms and molecules, and ultrabroadband attosecond pulses can simultaneously cover multiple absorption edges in atoms, molecules and complex materials. However, application of such pulses remains challenging because of the low spectral and temporal resolution of traditional photoelectron spectroscopy. In this section, we discuss recent experimental progress in using novel techniques to improve the temporal and spectral resolution; ultrabroadband isolated attosecond pulses are directly applicable to such techniques.

Bound-state wave-packet dynamics. The spectrum of a broadband isolated attosecond pulse can simultaneously cover bound (or quasi-bound) and continuum states of an atom or molecule, resulting in

the formation of a wave packet consisting of both bound and continuum states, which naturally evolves on attosecond timescales. A delayed NIR laser can then transfer population between bound states or ionize the excited states, promoting bound electrons to the continuum. The wave-packet dynamics can be probed using attosecond electron interferometry[82,83] or attosecond transient absorption spectroscopy[84,85].

After the initial excitation of the target by the attosecond pulse, both the bound and continuum wave packets evolve freely. The subsequent ionization of the excited states by the NIR laser results in a second, delayed continuum wave packet, as illustrated schematically in Fig. 4a. As the time delay between the attosecond and NIR laser pulses is varied, the interference of the two wave packets is manifested in delay-dependent oscillations of the electron spectrum. In analogy to quantum-state holography[86], this interference can be classified as being between a reference wave packet (directly ionized by the attosecond pulse) and an object wave packet (delayed ionization of the bound wave packet by the NIR laser); the full complex amplitude, including the lifetime and phase, of each excited state in the bound wave packet can be extracted. Such a measurement was recently performed in singly excited states of helium atoms[82], but it is applicable to more general systems as well.

Analogous experiments using transient absorption spectroscopy can similarly reveal the dynamics in bound wave packets (Fig. 4b). In transient absorption, instead of measuring photoelectrons, the attosecond pulse is spectrally dispersed after interaction with the target. Again, scanning the time delay produces interference oscillations in the transmitted spectrum[87–90], which are analogous to the quantum path interferences in the photoelectron measurements[82]. Additionally, the transient absorption experiments reveal several features that arise from bound–bound couplings and are absent in electron interferometry measurements, such as the effects of the instantaneous a.c. Stark shifts[91] and the formation of light-induced states[92]. In addition to the experiments in singly excited states of helium, wave-packet interferences have also been observed in transient absorption of singly excited neon[93] and doubly excited helium[94], and experiments are currently underway in molecules[95].

Correlated electron motion. In general, attosecond transient absorption appears to be a promising tool for the application of ultrabroadband attosecond pulses to the study of electron correlation in atoms[85,94,96] and more complex targets[97]. Very recently, attosecond transient absorption has been applied to study field-induced insulating-to-conducting state transitions in SiO_2 glass exposed to a strong laser field[98]. Experiments[99] revealed instantaneous and reversible field-induced modification of the insulating material, by probing changes in the transmission of the glass in the vicinity of the L-shell excitonic transition (~100 eV) of silicon. The results have tremendous implications for the development of lightwave electronics[100], and indicate that transient absorption spectroscopy may allow the first access to time-resolved processes and ultrafast switching in high-T_c superconductors or semiconductor solar cells with ultrabroadband isolated attosecond pulses that can cover the absorption edges of all the constituent atoms.

Conclusion and future outlook

Laser technology for the development of ultrabroadband attosecond light sources is rapidly maturing, and when combined with suitable attosecond pulse compression techniques, will soon lead to diverse sources of single-cycle attosecond pulses covering plateau and cutoff harmonics spanning the XUV and SXR spectral regions. Such pulses are ideally suited for applications in attosecond electron interferometry and attosecond transient absorption spectroscopy. By extending such attosecond sources and spectroscopic techniques to kiloelectronvolt photon energies, the potential of attosecond

technology for studying electron correlation in complex materials can be realized. Finally, combining the techniques used to generate broadband attosecond pulses with those for generating high-energy isolated attosecond pulses will allow for the generation of single-cycle pulses with gigawatt peak powers and petawatt per square centimetre peak intensities at the target, which can be applied in true attosecond-pump/attosecond-probe experiments.

References

1. Hentschel, M. *et al*. Attosecond metrology. *Nature* **414**, 509–513 (2001).
2. Nisoli, M. *et al*. Compression of high-energy laser pulses below 5 fs. *Opt. Lett.* **22**, 522–524 (1997).
3. Chang, Z. & Corkum, P. Attosecond photon sources: the first decade and beyond [Invited]. *J. Opt. Soc. Am. B* **27**, B9–B17 (2010).
4. Zhao, K. *et al*. Tailoring a 67 attosecond pulse through advantageous phase-mismatch. *Opt. Lett.* **37**, 3891–3893 (2012).
5. Mashiko, H. *et al*. Extreme ultraviolet supercontinua supporting pulse durations of less than one atomic unit of time. *Opt. Lett.* **34**, 3337–3339 (2009).
6. Sansone, G. *et al*. Isolated single-cycle attosecond pulses. *Science* **314**, 443–446 (2006).
7. Goulielmakis, E. *et al*. Single-cycle nonlinear optics. *Science* **320**, 1614–1617 (2008).
8. Yost, D. C. *et al*. Vacuum-ultraviolet frequency combs from below-threshold harmonics. *Nature Phys.* **5**, 815–820 (2009).
9. Power, E. P. *et al*. XFROG phase measurement of threshold harmonics in a Keldysh-scaled system. *Nature Photon.* **4**, 352–356 (2010).
10. Chang, Z., Rundquist, A., Wang, H., Murnane, M. M. & Kapteyn, H. C. Generation of coherent soft X rays at 2.7 nm using high harmonics. *Phys. Rev. Lett.* **79**, 2967–2970 (1997).
11. Spielmann, C. *et al*. Generation of coherent X-rays in the water window using 5-femtosecond laser pulses. *Science* **278**, 661–664 (1997).
12. Shan, B. & Chang, Z. Dramatic extension of the high-order harmonic cutoff by using a long-wavelength driving field. *Phys. Rev. A* **65**, 011804(R) (2001).
13. Popmintchev, T. *et al*. Bright coherent ultrahigh harmonics in the keV X-ray regime from mid-infrared femtosecond lasers. *Science* **336**, 1287–1291 (2012).
14. Corkum, P. B. & Krausz, F. Attosecond science. *Nature Phys.* **3**, 381–387 (2007).
15. Krausz, F. & Ivanov, M. Attosecond physics. *Rev. Mod. Phys.* **81**, 163–234 (2009).
16. Sansone, G., Poletto, L. & Nisoli, M. High-energy attosecond light sources. *Nature Photon.* **5**, 655–663 (2011).
17. Baltuška, A. *et al*. Attosecond control of electronic processes by intense light fields. *Nature* **421**, 611–615 (2003).
18. Nisoli, M. *et al*. Effects of carrier-envelope phase differences of few-optical-cycle light pulses in single-shot high-order-harmonic spectra. *Phys. Rev. Lett.* **91**, 213905 (2003).
19. Haworth, C. A. *et al*. Half-cycle cutoffs in harmonic spectra and robust carrier-envelope phase retrieval. *Nature Phys.* **3**, 52–57 (2007).
20. Kienberger, R. *et al*. Atomic transient recorder. *Nature* **427**, 817–821 (2004).
21. Witting, T. *et al*. Sub-4-fs laser pulse characterization by spatially resolved spectral shearing interferometry and attosecond streaking. *J. Phys. B* **45**, 074014 (2012).
22. Jullien, A. *et al*. Ionization phase-match gating for wavelength-tunable isolated attosecond pulse generation. *Appl. Phys. B* **93**, 433–442 (2008).
23. Abel, M. J. *et al*. Isolated attosecond pulses from ionization gating of high-harmonic emission. *Chem. Phys.* **366**, 9–14 (2009).
24. Thomann, I. *et al*. Characterizing isolated attosecond pulses from hollow-core waveguides using multi-cycle driving pulses. *Opt. Express* **17**, 4611–4633 (2009).
25. Ferrari, F. *et al*. High-energy isolated attosecond pulses generated by above-saturation few-cycle fields. *Nature Photon.* **4**, 875–879 (2010).
26. Corkum, P. B., Burnett, N. H. & Ivanov, M. Y. Subfemtosecond pulses. *Opt. Lett.* **19**, 1870–1872 (1994).
27. Sola, I. J. *et al*. Controlling attosecond electron dynamics by phase-stabilized polarization gating. *Nature Phys.* **2**, 319–322 (2006).
28. Mashiko, H. *et al*. Double optical gating of high-order harmonic generation with carrier-envelope phase stabilized lasers. *Phys. Rev. Lett.* **100**, 103906 (2008).
29. Feng, X. *et al*. Generation of isolated attosecond pulses with 20 to 28 femtosecond lasers. *Phys. Rev. Lett.* **103**, 183901 (2009).
30. Mashiko, H. *et al*. Tunable frequency-controlled isolated attosecond pulses characterized by either 750 nm or 400 nm wavelength streak fields. *Opt. Express* **18**, 25887–25895 (2010).
31. Vincenti, H. & Quéré, F. Attosecond lighthouses: how to use spatiotemporally coupled light fields to generate isolated attosecond pulses. *Phys. Rev. Lett.* **108**, 113904 (2012).
32. Kim, K. T. *et al*. Photonic streaking of attosecond pulse trains. *Nature Photon.* **7**, 651–656 (2013).
33. Wirth, A. *et al*. Synthesized light transients. *Science* **334**, 195–200 (2011).
34. Hassan, M. Th. *et al*. Invited article: attosecond photonics: synthesis and control of light transients. *Rev. Sci. Instrum.* **83**, 111301 (2012).
35. Corkum, P. B. Plasma perspective on strong field multiphoton ionization. *Phys. Rev. Lett.* **71**, 1994–1997 (1993).
36. Budil, K. S., Salières, P., L'Huillier, A., Ditmire, T. & Perry, M. D. Influence of ellipticity on harmonic generation. *Phys. Rev. A* **48**, R3437–R3440 (1993).
37. Möller, M. *et al*. Dependence of high-order-harmonic-generation yield on driving-laser ellipticity. *Phys. Rev. A* **86**, 011401(R) (2012).
38. Sansone, G. *et al*. Shaping of attosecond pulses by phase-stabilized polarization gating. *Phys. Rev. A* **80**, 063837 (2009).
39. Marceau, C., Gingras, G. & Witzel, B. Continuously adjustable gate width setup for attosecond polarization gating: theory and experiment. *Opt. Express* **19**, 3576–3591 (2011).
40. Strelkov, V. *et al*. Single attosecond pulse production with an ellipticity-modulated driving IR pulse. *J. Phys. B* **38**, L161–L167 (2005).
41. Sansone, G. *et al*. Towards atomic unit pulse duration by polarization-controlled few-cycle pulses. *J. Phys. B* **42**, 134005 (2009).
42. Mauritsson, J. *et al*. Attosecond pulse trains generated using two color laser fields. *Phys. Rev. Lett.* **97**, 013001 (2006).
43. Oishi, Y., Kaku, M., Suda, A., Kannari, F. & Midorikawa, K. Generation of extreme ultraviolet continuum radiation driven by a sub-10-fs two-color field. *Opt. Express* **14**, 7230–7237 (2006).
44. Tzallas, P. *et al*. Generation of intense continuum extreme-ultraviolet radiation by many-cycle laser fields. *Nature Phys.* **3**, 846–850 (2007).
45. Skantzakis, E., Tzallas, P., Kruse, J., Kalpouzos, C. & Charalambidis, D. Coherent continuum extreme ultraviolet radiation in the sub-100-nJ range generated by a high-power many-cycle laser field. *Opt. Lett.* **34**, 1732–1734 (2009).
46. Mashiko, H., Oguri, K. & Sogawa, T. Attosecond pulse generation in carbon K-edge region (284 eV) with sub-250 μJ driving laser using generalized double optical gating method. *Appl. Phys. Lett.* **102**, 171111 (2013).
47. Wu, Y. *et al*. Generation of high-flux attosecond extreme ultraviolet continuum with a 10 TW laser. *Appl. Phys. Lett.* **102**, 201104 (2013).
48. Wheeler, J. A. *et al*. Attosecond lighthouses from plasma mirrors. *Nature Photon.* **6**, 829–833 (2012).
49. Colosimo, P. *et al*. Scaling strong-field interactions towards the classical limit. *Nature Phys.* **4**, 386–389 (2008).
50. Schmidt, B. E. *et al*. High harmonic generation with long-wavelength few-cycle laser pulses. *J. Phys. B* **45**, 074008 (2012).
51. Doumy, G. *et al*. Attosecond synchronization of high-order harmonics from midinfrared drivers. *Phys. Rev. Lett.* **102**, 093002 (2009).
52. Takahashi, E. J., Kanai, T., Ishikawa, K. L., Nabekawa, Y. & Midorikawa, K. Coherent water window X ray by phase-matched high-order harmonic generation in neutral media. *Phys. Rev. Lett.* **101**, 253901 (2008).
53. Popmintchev, T. *et al*. Phase matching of high harmonic generation in the soft and hard X-ray regions of the spectrum. *Proc. Natl Acad. Sci.* **106**, 10516–10521 (2009).
54. Vozzi, C. *et al*. Millijoule-level phase-stabilized few-optical-cycle infrared parametric source. *Opt. Lett.* **32**, 2957–2959 (2007).
55. Gu, X. *et al*. Generation of carrier-envelope-phase-stable 2-cycle 740-μJ pulses at 2.1-μm carrier wavelength. *Opt. Express* **17**, 62–69 (2009).
56. Mücke, O. D. *et al*. Self-compression of millijoule 1.5 μm pulses. *Opt. Lett.* **34**, 2498–2500 (2009).
57. Andriukaitis, G. *et al*. 90 GW peak power few-cycle mid-infrared pulses from an optical parametric amplifier. *Opt. Lett.* **36**, 2755–2757 (2011).
58. Schmidt, B. E. *et al*. CEP stable 1.6 cycle laser pulses at 1.8 μm. *Opt. Express* **19**, 6858–6864 (2011).
59. Silva, F., Bates, P. K., Esteban-Martin, A., Ebrahim-Zadeh, M. & Biegert, J. High-average-power, carrier-envelope phase-stable, few-cycle pulses at 2.1 μm from a collinear BiB$_3$O$_6$ optical parametric amplifier. *Opt. Lett.* **37**, 933–935 (2012).
60. Shiner, A. D. *et al*. Probing collective multi-electron dynamics in xenon with high-harmonic spectroscopy. *Nature Phys.* **7**, 464–467 (2011).
61. Ishii, N. *et al*. Generation of soft x-ray and water window harmonics using a few-cycle, phase-locked, optical parametric chirped-pulse amplifier. *Opt. Lett.* **37**, 97–99 (2012).
62. Mairesse, Y. & Quéré, F. Frequency-resolved optical gating for complete reconstruction of attosecond bursts. *Phys. Rev. A* **71**, 011401(R) (2005).
63. Chini, M., Gilbertson, S., Khan, S. D. & Chang, Z. Characterizing ultrabroadband attosecond lasers. *Opt. Express* **18**, 13006–13016 (2010).

64. Gagnon, J., Goulielmakis, E. & Yakovlev, V. S. The accurate FROG characterization of attosecond pulses from streaking measurements. *Appl. Phys. B* **92,** 25–32 (2008).
65. Wang, H. *et al.* Practical issues of retrieving isolated attosecond pulses. *J. Phys. B* **42,** 134007 (2009).
66. Paul, P. M. *et al.* Observation of a train of attosecond pulses from high harmonic generation. *Science* **292,** 1689–1692 (2001).
67. Chen, C.-C., Chen, Y.-S., Huang, C.-B., Chen, M.-C. & Yang, S.-D. Noniterative data inversion of phase retrieval by omega oscillating filtering for optical arbitrary waveform measurement. *Opt. Lett.* **38,** 2011–2013 (2013).
68. Laurent, G., Cao, W., Ben-Itzhak, I. & Cocke, C. L. Attosecond pulse characterization. *Opt. Express* **21,** 16914–16927 (2013).
69. Dudovich, N. *et al.* Measuring and controlling the birth of attosecond XUV pulses. *Nature Phys.* **2,** 781–786 (2006).
70. Bertrand, J. B. *et al.* Ultrahigh-order wave mixing in noncollinear high harmonic generation. *Phys. Rev. Lett.* **106,** 023001 (2011).
71. Dahlström, J. M. *et al.* Atomic and macroscopic measurements of attosecond pulse trains. *Phys. Rev. A* **80,** 033836 (2009).
72. Kim, K. T. *et al.* Manipulation of quantum paths for space–time characterization of attosecond pulses. *Nature Phys.* **9,** 159–163 (2013).
73. Kohler, M. C., Keitel, C. H. & Hatsagortsyan, K. Z. Attochirp-free high-order harmonic generation. *Opt. Express* **19,** 4411–4420 (2011).
74. Serrat, C. Broadband spectral-phase control in high-order harmonic generation. *Phys. Rev. A* **87,** 013825 (2013).
75. Kim, K. T., Kim, C. M., Baik, M.-G., Umesh, G. & Nam, C. H. Single sub-50-attosecond pulse generation from chirp-compensated harmonic radiation using material dispersion. *Phys. Rev. A* **69,** 051805(R) (2004).
76. Ko, D. H., Kim, K. T. & Nam, C. H. Attosecond-chirp compensation with material dispersion to produce near transform-limited attosecond pulses. *J. Phys. B* **45,** 074015 (2012).
77. Morlens, A.-S. *et al.* Compression of attosecond harmonic pulses by extreme-ultraviolet chirped mirrors. *Opt. Lett.* **30,** 1554–1556 (2005).
78. Morlens, A.-S. *et al.* Design and characterization of extreme-ultraviolet broadband mirrors for attosecond science. *Opt. Lett.* **31,** 1558–1560 (2006).
79. Hofstetter, M. *et al.* Attosecond dispersion control by extreme ultraviolet multilayer mirrors. *Opt. Express* **19,** 1767–1776 (2011).
80. Guggenmos, A. *et al.* Aperiodic CrSc multilayer mirrors for attosecond water window pulses. *Opt. Express* **21,** 21728–21740 (2013).
81. Bourassin-Bouchet, C. *et al.* Shaping of single-cycle sub-50-attosecond pulses with multilayer mirrors. *New J. Phys.* **14,** 023040 (2012).
82. Mauritsson, J. *et al.* Attosecond electron spectroscopy using a novel interferometric pump-probe technique. *Phys. Rev. Lett.* **105,** 053001 (2010).
83. Choi, N. N., Jiang, T. F., Morishita, T., Lee, M.-H. & Lin, C. D. Theory of probing attosecond electron wave packets via two-path interference of angle-resolved photoelectrons. *Phys. Rev. A* **82,** 013409 (2010).
84. Goulielmakis, E. *et al.* Real-time observation of valence electron motion. *Nature* **466,** 739–743 (2010).
85. Wang, H. *et al.* Attosecond time-resolved autoionization of argon. *Phys. Rev. Lett.* **105,** 143002 (2010).
86. Klünder, K. *et al.* Reconstruction of attosecond electron wave packets using quantum state holography. *Phys. Rev. A* **88,** 033404 (2013).
87. Chen, S. *et al.* Light-induced states in attosecond transient absorption spectra of laser-dressed helium. *Phys. Rev. A* **86,** 063408 (2012).
88. Chini, M. *et al.* Sub-cycle oscillations in virtual states brought to light. *Sci. Rep.* **3,** 1105 (2013).
89. Gallmann, L. *et al.* Resolving intra-atomic electron dynamics with attosecond transient absorption spectroscopy. *Mol. Phys.* **111,** 2243–2250 (2013).
90. Chen, S., Wu, M., Gaarde, M. B. & Schafer, K. J. Quantum interference in attosecond transient absorption of laser-dressed helium atoms. *Phys. Rev. A* **87,** 033408 (2013).
91. Chini, M. *et al.* Subcycle ac Stark shift of helium excited states probed with isolated attosecond pulses. *Phys. Rev. Lett.* **109,** 073601 (2012).
92. Bell, M. J., Beck, A. R., Mashiko, H., Neumark, D. M. & Leone, S. R. Intensity dependence of light-induced states in transient absorption of laser-dressed helium measured with isolated attosecond pulses. *J. Mod. Opt.* **60,** 1506–1516 (2013).
93. Wang, X. *et al.* Subcycle laser control and quantum interferences in attosecond photoabsorption of neon. *Phys. Rev. A* **87,** 063413 (2013).
94. Ott, C. *et al.* Quantum interferometry and correlated two-electron wave-packet observation in helium. Preprint at http://arXiv.org/abs/1205.0519 (2012).
95. Sansone, G. *et al.* Attosecond absorption spectroscopy in molecules. Paper QF2C.1 in *CLEO-QELS – Fundamental Science* (OSA, 2013).
96. Ott, C. *et al.* Lorentz meets fano in spectral line shapes: a universal phase and its laser control. *Science* **340,** 716–720 (2013).
97. Moskalenko, A. S., Pavlyukh, Y. & Berakdar, J. Attosecond tracking of light absorption and refraction in fullerenes. *Phys. Rev. A* **86,** 013202 (2012).
98. Schiffrin, A. *et al.* Optical-field-induced current in dielectrics. *Nature* **493,** 70–74 (2013).
99. Schultze, M. *et al.* Controlling dielectrics with the electric field of light. *Nature* **493,** 75–78 (2013).
100. Goulielmakis, E. *et al.* Attosecond control and measurement: lightwave electronics. *Science* **317,** 769–775 (2007).

Acknowledgements

Additional information

Reprints and permissions information is available at www.nature.com/reprints. Requests for materials and correspondence should be addressed to Z.C.

Competing financial interests

The authors declare no competing financial interests.